

NASA Technical Memorandum 102358  
AIAA-89-2910

# Engine Inlet Distortion in a 9.2 Percent Scale Vectored Thrust STOVL Model in Ground Effect

Albert L. Johns and George Neiner  
*Lewis Research Center*  
*Cleveland, Ohio*

and

J.D. Flood, K.C. Amuedo, and T.W. Strock  
*McDonnell Douglas Corporation*  
*St. Louis, Missouri*

Prepared for the  
25th Joint Propulsion Conference  
cosponsored by the AIAA, ASME, SAE, and ASEE  
Monterey, California, July 10-12, 1989



(NATA-1M-102358) ENGINE INLET DISTORTION IN  
A 9.2 PERCENT SCALE VECTORED THRUST STOVL  
MODEL IN GROUND EFFECT (NASA) 24 DCSC 01A

NPO-17561

Unclas  
G3/02 0266113



# ENGINE INLET DISTORTION IN A 9.2 PERCENT SCALED VECTORED THRUST

## STOVL MODEL IN GROUND EFFECT

Albert L. Johns and George Neiner  
National Aeronautics and Space Administration  
Lewis Research Center  
Cleveland, Ohio 44135

and

J.D. Flood, K.C. Amuedo, and T.W. Strock  
McDonnell Aircraft Company  
McDonnell Douglas Corporation  
St. Louis, Missouri 63166

## SUMMARY

Advanced Short Takeoff/Vertical Landing (STOVL) aircraft which can operate from remote locations, damaged runways, and small air capable ships are being pursued for deployment around the turn of the century. To achieve this goal, NASA Lewis Research Center, McDonnell Douglas Aircraft, and DARPA defined a cooperative program for testing in the NASA Lewis 9- by 15-Foot Low Speed Wind Tunnel (LSWT) to establish a database for hot gas ingestion, one of the technologies critical to STOVL. This paper will present results showing the engine inlet distortions (both temperature and pressure) in a 9.2 percent scale Vectored Thrust STOVL model in ground effects. Results are shown for the forward nozzle splay angles of  $0^\circ$ ,  $-6^\circ$ , and  $18^\circ$ . The model support system had  $4^\circ$  of freedom, heated high pressure air for nozzle flow, and a suction system exhaust for inlet flow. The headwind (freestream) velocity was varied from 8 to 23 kn.

## INTRODUCTION

Advanced Short Takeoff and Vertical Landing (STOVL) aircrafts are being considered for operation around the turn of the century. In order to meet this time frame, it is necessary that the technology critical to the successful operation of the STOVL concepts be resolved. One of the critical technology items associated with the vectored thrust concept is that of hot gas ingestion while the aircraft is in ground effect (refs. 1 and 2). Hot gas ingestion occurs when the hot exhaust jet hits the ground and radiates in all directions until it encounters another jet. When the jets meet a fountain is formed. This fountain can hit the undersurface of the fuselage and run forward into the inlet flow field. The hot air, once ingested, can result in both compressor temperature and pressure distortions and loss in engine thrust and/or stall.

Hot gas ingestion can be categorized as near field and far field phenomena. The near field hot gas problem results from the hot exhaust jet impinging on the undersurface of the model due to the jet fountain. The jet fountain is formed by the jet (from each nozzle) which flows in all directions. When one jet encounters another, the air flows upward forming a fountain which, if under the fuselage, will interact with the fuselage and can flow forward (along the fuselage) into the inlet intake region. The near field hot gas ingestion is

generally the primary source of the hot gas ingestion. The near field hot gas ingestion is a function of the model height above the ground plane (ref. 2). The far field hot gas ingestion occurs when the ground jet flow separates from the ground ahead of the model and gets blown back into the inlet flow field. The far field hot gas ingestion is a function of the headwind. The magnitude of the far hot gas ingestion is greatly reduced in comparison to the near field.

This paper will present results of the engine inlet distortions (both temperature and pressure) in a 9.2 percent scale Vectored Thrust STOVL model in ground effects. The effects of forward nozzle splay on the ground plane and model surfaces are also presented. Results are shown for the forward nozzle splay angles of  $0^\circ$ ,  $-6^\circ$ , and  $18^\circ$ . The STOVL models required a unique model support system. The model support system had four-degrees of freedom; pitch, roll, yaw, and vertical height variation, heated high pressure air for nozzle flow, and a suction system exhaust for inlet flow. The primary hot gas ingestion testing was conducted over a headwind (freestream) velocity ranging from 8 to 23 kn. Several configurations were tested from 5 to 85 kn.

#### FACILITY, MODEL CONFIGURATIONS AND SUPPORT SYSTEM

The NASA Lewis 9- by 15-Foot Low Speed Wind Tunnel (LSWT) was used to develop the hot gas ingestion database. The 9- by 15-Foot LSWT, constructed within the return leg of the 8- by 6-Foot Supersonic Wind Tunnel (SWT), is shown schematically in figure 2. Tunnel velocities from 30 to 90 kn were set by using the compressor and number 1 and 2 doors. Tunnel velocities from 8 to 23 kn were set by using the air dryer blowers and number 4 and 5 doors.

A schematic for the HGI model, 279-3C, is shown in figure 3 consisting of five major subassemblies; the forward fuselage, center fuselage, aft fuselage, the wings, and canards. The forward fuselage contained the main inlet and a translating cowl auxiliary inlet which makes up the bifurcated inlet system. The inlet suction duct is part of the suction system and was used to create inlet (compressor face) flow. The center fuselage contained the nozzle system, and high pressure hot air lines supplied the hot air to the model's four nozzles. Lift improvement devices were also attached to the center fuselage.

The undersurface of the HGI model with the  $18^\circ$  splay and  $-6^\circ$  splay configurations are shown in figure 4. Also shown are the Lift Improvement Devices (LIDs) installed on the  $18^\circ$  splay configuration. The LIDs consist of longitudinal strakes, sidewalls, forward fence and aft fence(optional). The LIDs generally enclosed the forward and aft pair nozzles.

The definition of the forward nozzle splay angle is shown in figure 5(a). The splay angle is measured with reference to a vertical line through the nozzle centerline. A negative splay means the nozzles are in-board of the vertical line. A positive splay means the nozzles are out-board of the vertical line.

This presentation will show results from three different forward nozzle splay angles,  $-6^\circ$ ,  $0^\circ$ , and  $18^\circ$ .

The nozzle vector thrust angle is shown in figure 5(b). The nozzle vector angle for the data presented in this paper is  $82^\circ$  on the forward nozzles and

84° on the aft nozzles. The model was capable of vectoring thrust from 0° (full aft) to 110° (slightly forward).

#### MODEL INSTALLED IN THE 9-BY 15-FOOT LOW SPEED WIND TUNNEL

The installation of a 9.2 percent scaled model and the supporting systems in the 9- By 15-Foot Low Speed Wind Tunnel are shown in figure 6. The supporting systems included the model support with 4° of freedom; pitch, roll, yaw, and vertical height adjustment. A ground plane was installed with static pressure, air temperature instrumentation, and boundary layer rakes. The ground plane had a sliding trap door. The trap door was open when the nozzle conditions were being set and closed to setup the steady state conditions during data recording. Figure 7, an aft view of the 9- by 15-ft LSWT shows the ground plane ejector system which evacuated the hot exhaust gases from the vicinity of model when the nozzle pressure ratios were being set. The ejectors were automatically shut off when the trap door closed.

A schematic of the ground plane is shown in figure 8. The ground plane was 336 in. long and 176 in. wide and was 18 in. off the wind tunnel floor. The trap door opening was 42 in. in the axial direction and 40.75 in. in the span direction. The trap door closed from a full open position in 0.5 sec.

A cross section view of the test section is show in figure 9. The test section is normally lined with an acoustic treatment. For the hot gas ingestion test, the floor treatment was removed and steel plates were installed as the tunnel floor. The ground plane system was attached to the steel floor. The treatment on the lower part of the walls was also removed so that the hot gases from the nozzles could flow out beyond the test section walls and mix with cooler air before entering the downstream diffuser section. A trap-door-scavenging system was located under the ground plane. When the nozzle pressure ratios are being set, the trap door is open, allowing the hot exhaust gases to exit the test section without heating the model, ground plane, and the local environment. When the trap door is closed, the lateral flow from the nozzle jets exit the test section through the sidewall bleed system (located on both the left and right sidewalls).

#### MODEL AND GROUND PLANE INSTRUMENTATIONS

The 9.2 percent scaled model of McDonnell concept 279-3C was instrumented along the underside of the fuselage, around the ramps and inlets (main and auxiliary), and also at the compressor face. The instrumentation consisted of static and total pressures, and protruding temperature probes (which measured the surface air temperature). The main objective of this paper is to present the results at the compressor face. Hence, the model instrumentation other than the compressor face will be shown on each figure which is pertinent. Figure 10 shows the compressor face rake instrumentation. Table I shows the location of each probe on the rake and the circumferential location. Each rake arm was made up of four total pressure and five total temperature measurements. One wall static pressure tap was located by each rake arm around the circumferential. Only steady state measurements were made during this test program.

The ground plane centerline instrumentation and the ground plane rakes are shown in figure 11. The centerline instrumentation consisted of static

pressures and flush mounted thermocouples (temperature taps) which were isolated from the plate surface so as to measure the ground plane air temperature. Table II shows the location of this instrumentation. There were three double sided instrumented rakes and two single sided instrumented rakes. The double sided rakes measured the freestream side flow and the flow coming from the nozzle jets (model side). The single sided rakes measured only the model side of the flow. There were two rake height, 4.0 and 11.0 in. Each rake contained total pressure, total temperature, and static pressure measurements. Additional instrumentation was located on the trap door and other section of the ground plane.

The test section airflow velocity measuring system is shown in figure 12. The anemometer was located on the test section ceiling near the entrance of the test section. The anemometer is capable of measuring velocities from 1 to 98 kn within  $\pm 0.6$  kn. The hot gas ingestion testing was generally conducted between velocities of 8 and 23 kn. However, several configurations were tested from 5 to 85 kn.

## RESULTS AND DISCUSSION

While it is the intent of this paper to present engine distortion data for an aircraft model in ground effect it is equally important to establish the environment that produced this distortion. Therefore, the influence of model height, nozzle splay, and lift improvement devices on the environment will be presented.

The data present in this section are for design condition as follows:

Forward nozzles pressure ratio . . . . .	3.02
Aft nozzles pressure ratio . . . . .	3.16
Model main landing gear height above the ground plane, in. . . . .	0.20
Compressor face Mach number . . . . .	0.40
Aft and Forward nozzles exhaust temperature, °F . . . . .	500
Headwind velocity, kn . . . . .	10
Model pitch angle, deg . . . . .	6.5
Model yaw angle, deg . . . . .	0
Model roll angle, deg . . . . .	0

In the text to follow, the above conditions have been referred to as "at design."

The effect of model height on the compressor face temperature rise is shown in figure 13 for forward nozzle splay angles of 0°, -6°, and 18°. In general, the -6° forward nozzle splay configuration had the lowest inlet temperature rise per model height above the ground plane. The forward nozzles are splayed inboard (minus splay) so that the two jets will form a single jet over a range of main landing gear heights above the ground plane. Merging the forward nozzle jets eliminates the fountain between the two forward nozzles. As a result, a reduction in the near field hot gas ingestion (HGI) occurs.

The first indication of ground effects occurs at the point where the compressor face temperature rise starts to increase with decreasing model height

above the ground plane. A comparison between the LIDs and clean configurations indicates that the  $-6^\circ$  forward nozzle splay ground effects started at the same ground height and only the magnitude of the compressor face temperature rise was different. This result should be anticipated in that the inboard splay tends to form a single jet over a range of model heights above the ground plane. The  $0^\circ$  forward splay showed different heights at which the ground effects began, 3 in. for the clean, and 1.5 in. when LIDs were installed. The  $18^\circ$  forward nozzle splay had a wider range in which ground effects occurred between the LIDs and clean configurations, 4.5 and 10 in. respectively. In general, the  $0^\circ$  forward nozzle splay configuration had a lower inlet temperature rise than the  $18^\circ$  forward nozzle splay configuration. The beginning of ground effects can be seen in figures 13(a) and (b), where the slope of each curve starts to slope upward, with decreasing model height. The reduction in the compressor face temperature rise between the clean configurations and LIDs indicate the effectiveness of the LIDs in controlling the near field fountain flow. In general, the same trends occurred for both the LIDs and the clean configurations. However, the magnitude of the compressor face temperature rise was greatly reduced.

The compressor face conditions can have an adverse effect on the normal operation of an aircraft particularly in the landing mode. An increase in the inlet temperature and/or pressure distortion can result in engine stall and an instantaneous loss in the nozzle thrust. Either of these can result in an aircraft failure while in ground effect. Therefore, when evaluating the model performance the distortion parameters becomes an essential ingredient. The distortions presented herein is the maximum-minus-minimum over the average for both the total pressure and total temperature at the compressor face. The compressor face temperature rise is the increase in compressor face temperature above the reference ambient temperature. The effect of forward nozzle splay on the compressor face parameters are shown in figure 14 without LIDs (fig. 14(a)) and with LIDs (fig. 14(b)) over a headwind velocity ranging from 5 to 23 kn ( $-6^\circ$  and  $0^\circ$  configuration), and 5 to 82 kn ( $18^\circ$  configuration). The highest pressure distortion (9.5 percent) occurred with the  $-6^\circ$  splay configuration and the lowest pressure distortion at (8 percent) with the  $0^\circ$  splay configuration.

The compressor face temperature distortion (fig. 14(a)) varied from 13 to 16 percent for the  $-6^\circ$  forward nozzle splay, 16 to 15 percent for the  $0^\circ$  splay, and 25 to 20 percent for the  $18^\circ$  splay configuration from a headwind velocity 5 to 25 kn. The temperature rise at the compressor face is also shown in figure 14(a). In general, this parameter is indicative of the compressor face temperature distortion.

Figure 14(b) presents the results when the lift improvement devices are added to the underside of the model. The compressor face pressure distortion is generally not affected by the LIDs. The  $0^\circ$  forward splay configuration compressor face pressure distortion increased from 8.0 percent (clean configuration) to 9.5 percent (with LIDs). However, the compressor face temperature distortion and inlet temperature rise, both decrease with the addition of LIDs. For example, the  $-6^\circ$  forward nozzle splay configuration compressor face distortion decreased from 15 to 3.5 percent at design. The  $0^\circ$  and  $18^\circ$  forward nozzle splay configurations decreased from 16 to 7 percent and 22 to 13 percent at design, respectively. The end result from the use of LIDs is to capture the fountain, thereby, reducing the near field hot gas ingestion contribution.

The effect of the forward nozzle splay on the model surface air temperature distribution is presented in figure 15(a) for the clean configurations. This figure shows the surface temperature distribution in the region of the main inlet plane and along the underside of the model at the centerline. The temperature distribution in the region of the main inlet is generally the same for the 0° and -6° splay configurations. The 18° splay configuration had an approximately 60 F° higher temperature in the main inlet region.

However, the undersurface of the model for the 18° splay was generally at a lower temperature than the 0° and -6° splay configuration. This is an indication that the fountain of the 18° splay configuration was less intensity. The undersurface air temperature distribution also indicates the region where the core fountain occurred. This region varied with each forward nozzle splay angle. The -6° and 0° splay configurations core fountain location occurred near model station 30 to 35. The 18° splay configuration, however, had a much larger axial region of maximum air temperature located 24 to 32 model stations ahead of the nozzles midpoint. This was an indication of a more diffused fountain and may account for the lower inlet temperature rise.

When LIDs were added (fig. 15(b)), the air temperature in the region of the main inlet was greatly reduced with the -6° splay configuration. For example, with the clean configuration, the air temperature was 240 °F (700 °R) and with LIDS, 100 °F (560 °R). A similar result occurred for the other configurations. However, one must keep in mind that the main inlet region is upstream of the LIDs. The undersurface air temperature distribution more clearly demonstrate the effectiveness of the LIDs, figures 15(a) and (b). The forward fence is located at station 22, and in general the air temperature distribution downstream of station 22 is identical to the clean configurations. However, upstream of model station 22 the air temperature is greatly reduced. The data also show an increase in the air temperature distribution, with the 18° splay configuration with LIDs.

The ground plane centerline surface air temperature and surface pressure change is shown in figure 16(a), clean configuration. In general, the air surface temperature along the ground plane centerline is very similar between the 0° and -6° forward nozzle splay configurations. Both configurations surface air temperature peak at a ground plane station of 3.0. However, the 18° forward nozzle splay configuration peak air temperature occurred at model station -4. The ground plane surface pressure change also reflects the difference in the forward nozzle splay configurations. The -6° and 0° forward nozzle splay configurations produced a negative pressure change on the ground plane up to 50 and 30 in. ahead of the mid-nozzle point, respectively. The 18° splay configuration had a region of positive pressure change.

The splay configurations with LIDs installed are shown in figure 16(b). In general, the surface air temperature distributions with LIDs are about the same as the without LIDs configurations. The only difference in air temperature distribution, on the ground plane, occurs only along the undersurface of the model with the LIDs installed.

The ground plane surface pressure change for the clean and LIDs configurations are shown in figures 16(a) and (b) respectively. Comparison of pressure data along the ground plane shows that the LIDs produced a positive pressure change only with the 18° splay. This can be seen in the surface pressures under the model and ahead of the mid-nozzle point. This positive surface



pressure change indicated that rather than the typical suckdown a lifting force was produced.

In order to get a better understanding on the inlet temperature rise and the total pressure recovery at the compressor face, figures 17 (a) and (b) shows the contour plots for both inlet pressure recovery and temperature rise. The clean configurations are shown in figure 17(a), for a 10 kn headwind, at design nozzle pressure ratio of 3.01, and a model main landing gear wheel height above the ground plane of 0.2. The maximum inlet rise, 82 F°, occurred with the forward nozzles in the 0° splay position. The -6° and 18° splay configurations both had a inlet temperature rise of 60 F°. As can be observed from figure 17(a), the contour plots for the -6° and 18° forward nozzle splay configurations look very similar. These two configurations had maximum inlet temperature rise of 60 F°. The 0° forward nozzle splay configuration temperature rise at the upper half of the compressor face varied from 90 to 160 F° and to 110 F° at the bottom of the compressor face. The 18° forward nozzle splay configuration compressor face temperature rise varied from 70 to 10 F° at the upper half to 120 F° at the bottom. The -6° forward nozzle splay configuration compressor face temperature rise varied from 120 to 30 F° at the upper half and from 120 to 90 F° in the lower half. In general, the 18° forward nozzle splay configuration had the cooler upper region (in the vicinity of the auxiliary inlets).

The contour plots for the total pressure recovery, figure 17, indicated a similar result as the temperature contours. The pressure recovery for the 18° forward nozzle splay configuration was 0.972, and 0.96 for both the 0° and -6° forward nozzle splay configurations. The 18°, 0°, and -6° forward nozzle splay configuration had the highest inlet recovery at the lower half of the compressor face.

The Lift Improvement Devices (LIDs) are generally used to capture the fountain when in ground effect and thereby improve the lift and off-setting the suckdown force. The LIDs can also serve in a second capacity, that is, a means of deflecting the hot exhaust jet away from the flow region which contains the inlet air flow. The addition of the LIDs on the clean configuration resulted in the contour plots shown in figure 17(b). In general, the inlet temperature rise was greatly reduced with LIDs. For example, the 18° forward nozzle splay configuration had the highest temperature rise at the compressor face, 33 F° above the reference temperature. The compressor face temperature rise for the 0° and -6° forward nozzle splay configurations were 22 and 8 F°, respectively.

The compressor face pressure recovery contour maps for LIDs configurations are also shown in figure 17(b). The largest loss in the compressor face total pressure recovery occurred at the upper half, in the vicinity of the auxiliary inlets. The lower section of the compressor face had a total pressure recovery ranging from 1.00 (-6°) to 0.98 (18° and 0°) forward nozzle splay configurations.

## SUMMARY OF RESULTS

Results showing the engine inlet distortions (pressure and temperature) on a 9.2 percent scale vectored thrust STOVL model in ground effects have been presented.

## General

1. The compressor face temperature rise and temperature distortion are a function of the model height above the ground plane and the forward nozzles splay angle.

2. Air temperature measurements along the underside of the model (when in ground effects) reflected the impingement of the core jet fountain.

3. Increasing the forward nozzle splay angle to  $18^\circ$  resulted in a higher air temperature distribution over 60 percent of the undersurface of the fuselage comparison to the  $-6^\circ$  and  $0^\circ$  forward nozzle splay configurations.

4. The  $-6^\circ$  and  $0^\circ$  forward nozzle splay configurations, in ground effects, resulted in a suckdown force on the ground plane. However, the forward nozzles with a  $18^\circ$  splay configuration and LIDs produced a positive pressure region on the ground plane under the model.

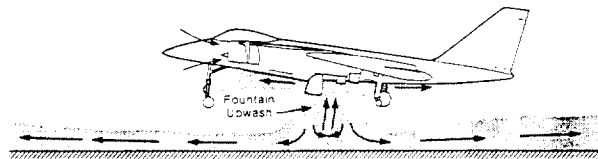
## Distortion

1. Both, the compressor face temperature rise and temperature distortion can be greatly reduced with Lift Improvement Devices (LIDs).

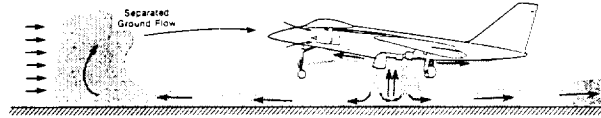
2. With the clean configurations, the hot gases generally entered the main inlets through the lower section causing the temperature distortion in the lower half of the compressor face.

## REFERENCES

1. Johns, A.L., et al.: Hot Gas Ingestion Testing of an Advanced STOVL Concept in the NASA Lewis 9- by 15-Foot Low Speed Wind Tunnel With Flow Visualization. NASA TM-100952, 1988 (also AIAA Paper 88-3025).
2. Amuedo, K.C., et al.: STOVL Hot Gas Ingestion Control Technology. ASME 89-GT-323, June 1989.



Near Field Hot Gas Ingestion Due to Fountain Upwash



Far Field Hot Gas Ingestion Due to Separated Ground Flow

FIGURE 1. - SOURCE OF HOT GAS INGESTION.

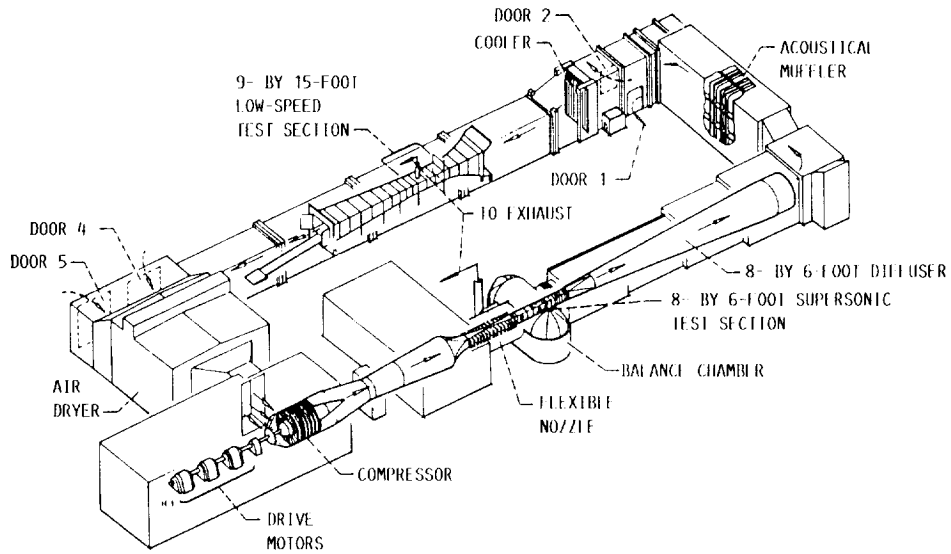


FIGURE 2. - AN ILLUSTRATION OF THE 9- BY 15-FOOT LOW-SPEED WIND TUNNEL AND THE 8- BY 6-FOOT SUPERSONIC WIND TUNNEL.

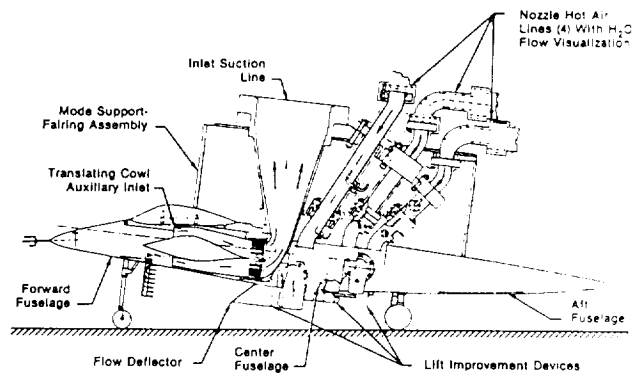


FIGURE 3. - SCHEMATIC OF MODEL 279-3C.

ORIGINAL PAGE  
BLACK AND WHITE PHOTOGRAPH

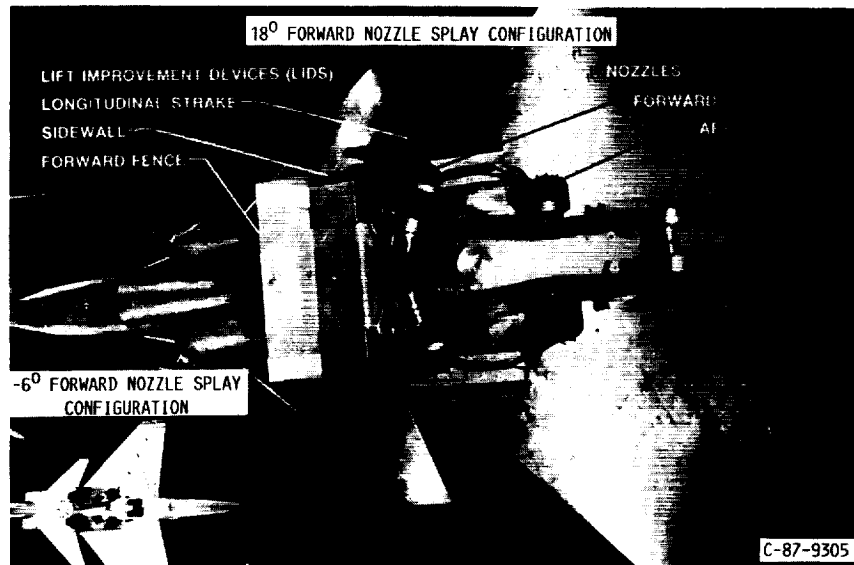


FIGURE 4. - UNDERSURFACE OF THE HGI MODEL SHOWING LIDS AND NOZZLES.

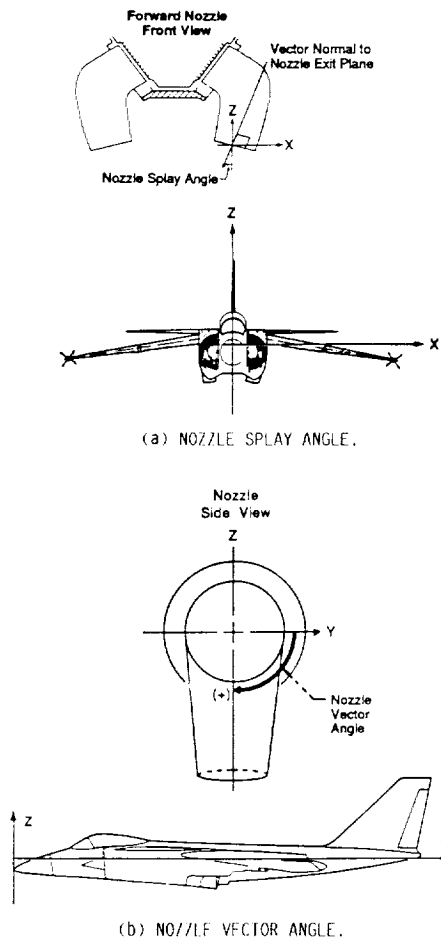


FIGURE 5. - DEFINITION OF FORWARD NOZZLES SPLAY AND VECTOR ANGLES.

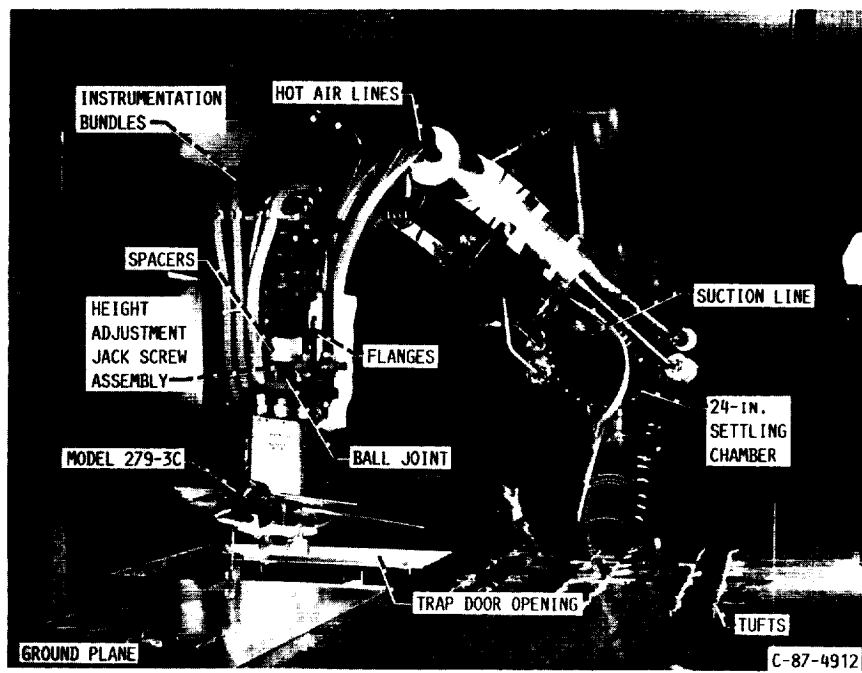


FIGURE 6. - HOT GAS INGESTION MODEL AND SUPPORTING SYSTEM INSTALLED IN THE 9- BY 15-FOOT LOW-SPEED WIND TUNNEL.

ORIGINAL PAGE  
BLACK AND WHITE PHOTOGRAPH



FIGURE 7. - AFT VIEW OF THE 9- BY 15-FOOT LOW-SPEED WIND TUNNEL TEST SECTION.

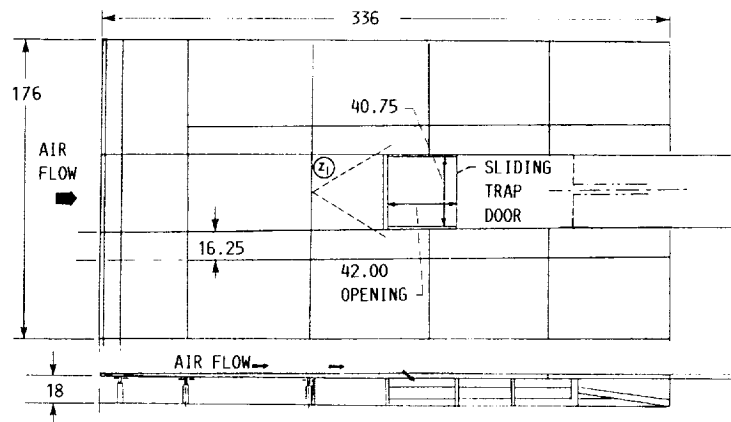


FIGURE 8. - SCHEMATIC OF THE GROUND PLANE. (DIMENSIONS IN INCHES).

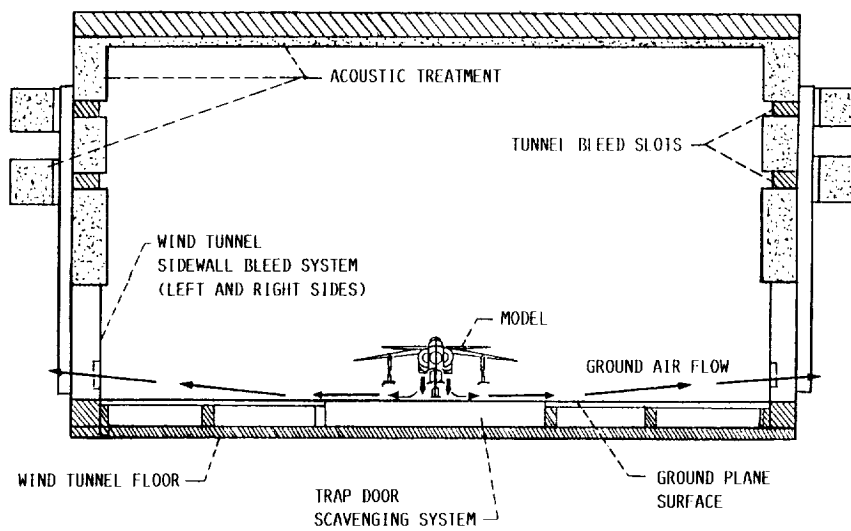


FIGURE 9. - CROSS SECTION OF THE TEST SECTION SHOWING THE SIDEWALLS BLEED AND TRAP DOOR SCAVENGING SYSTEMS.

LEG IDENTIFICATION			LEG IDENTIFICATION		
NUMBER	ANGLE, DEG	RADIUS, R, IN.	NUMBER	ANGLE, DEG	RADIUS, R, IN.
1	66.50		2	21.53	
4	293.50		3	338.47	
5	246.50		6	201.53	
8	113.50		7	158.47	
TOTAL TEMPERATURE		0.624	TOTAL TEMPERATURE		0.646
PRESSURE		0.698	PRESSURE		0.722
TEMPERATURE		1.081	TEMPERATURE		1.119
PRESSURE		1.209	PRESSURE		1.251
TEMPERATURE		1.396	TEMPERATURE		1.444
PRESSURE		1.560	PRESSURE		1.615
TEMPERATURE		1.651	TEMPERATURE		1.709
PRESSURE		1.810	PRESSURE		1.875
TEMPERATURE		1.872	TEMPERATURE		1.938
STATIC PRESSURE		2.038	STATIC PRESSURE		2.038

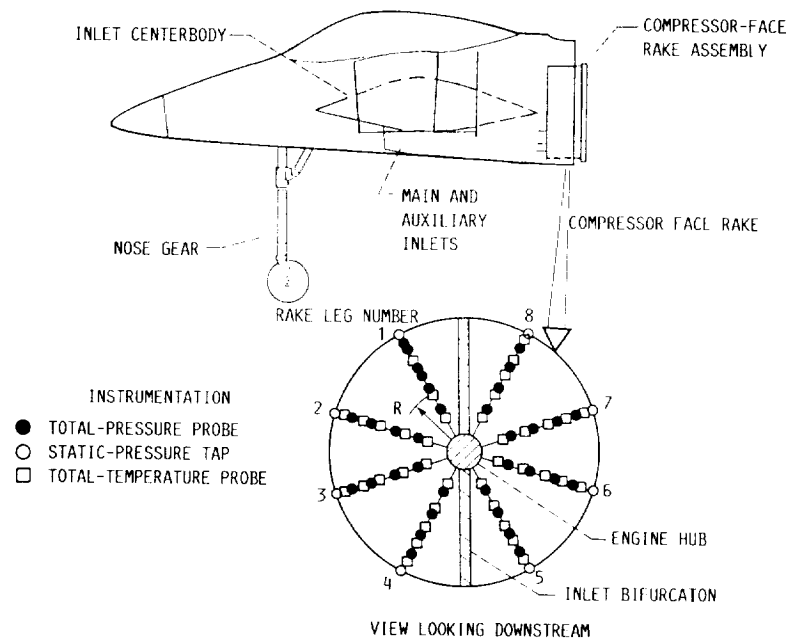


FIGURE 10. - COMPRESSOR FACE RAKE INSTRUMENTATION.

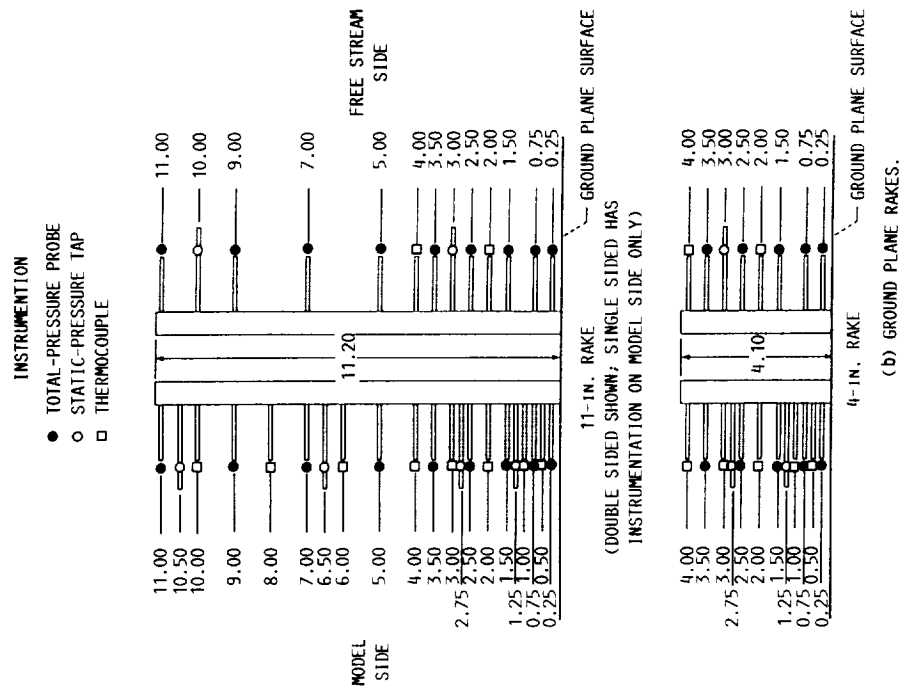


FIGURE 11. - GROUND PLANE INSTRUMENTATION. DIMENSIONS ARE IN INCHES.



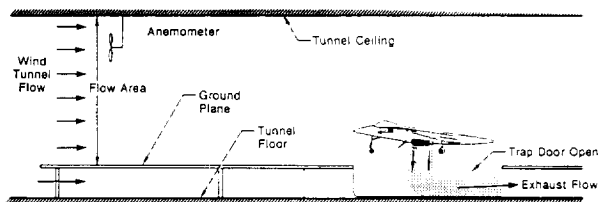
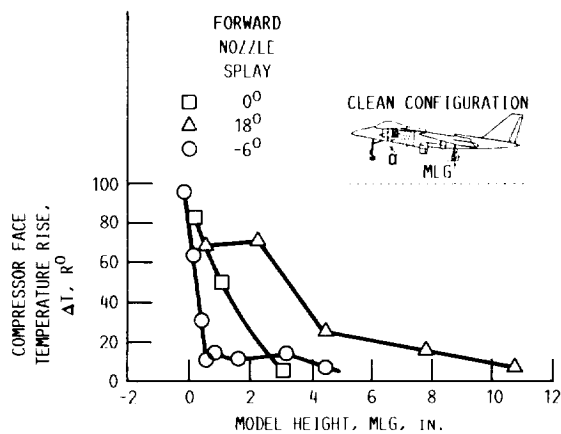
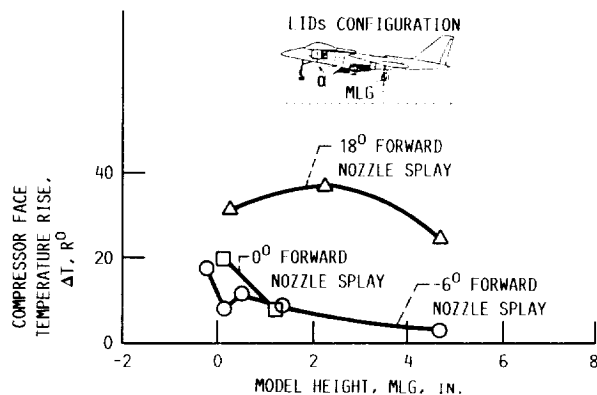


FIGURE 12. - TEST SECTION AIRFLOW VELOCITY MEASURING SYSTEM.



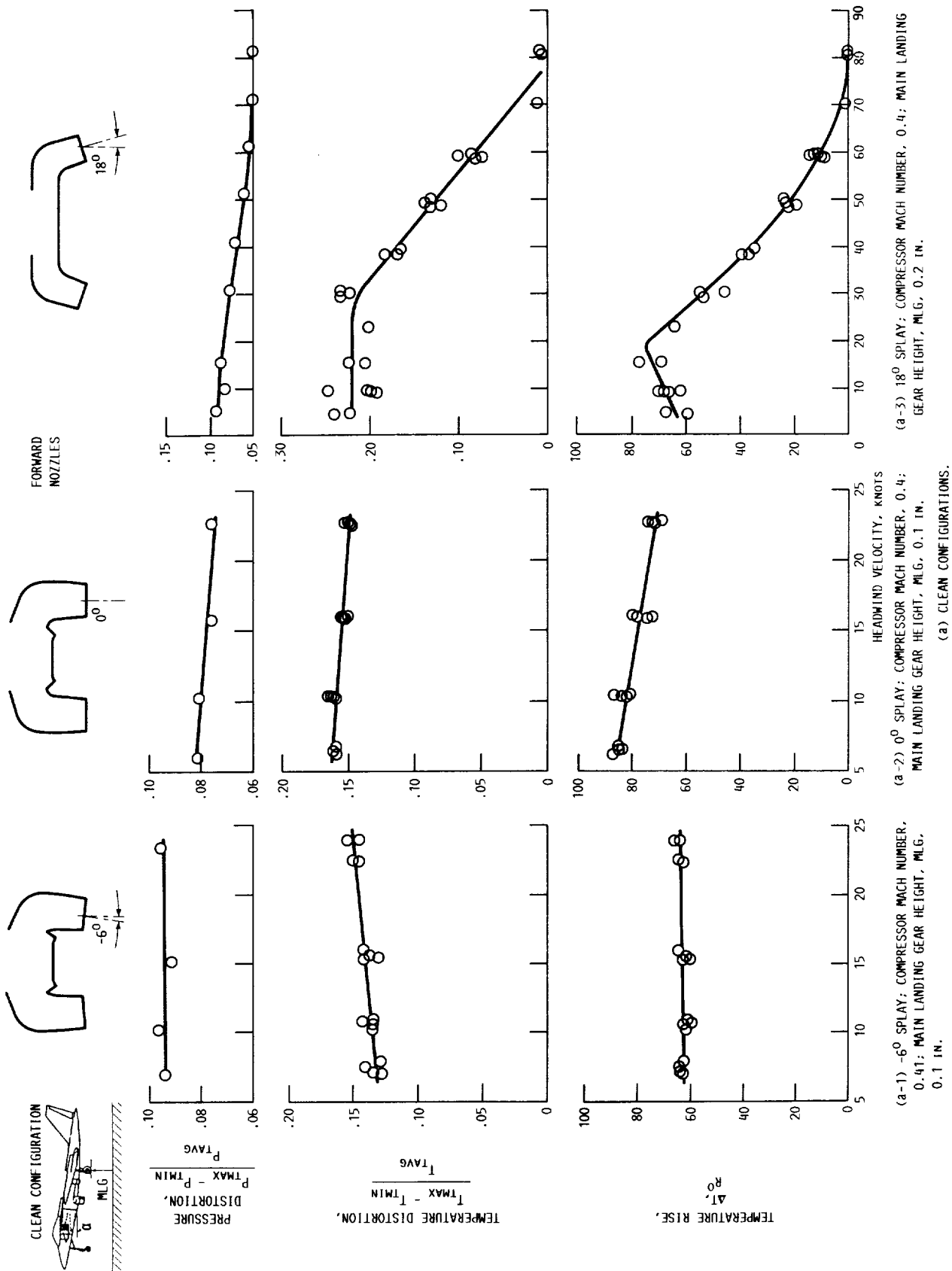
(a) CLEAN CONFIGURATION.

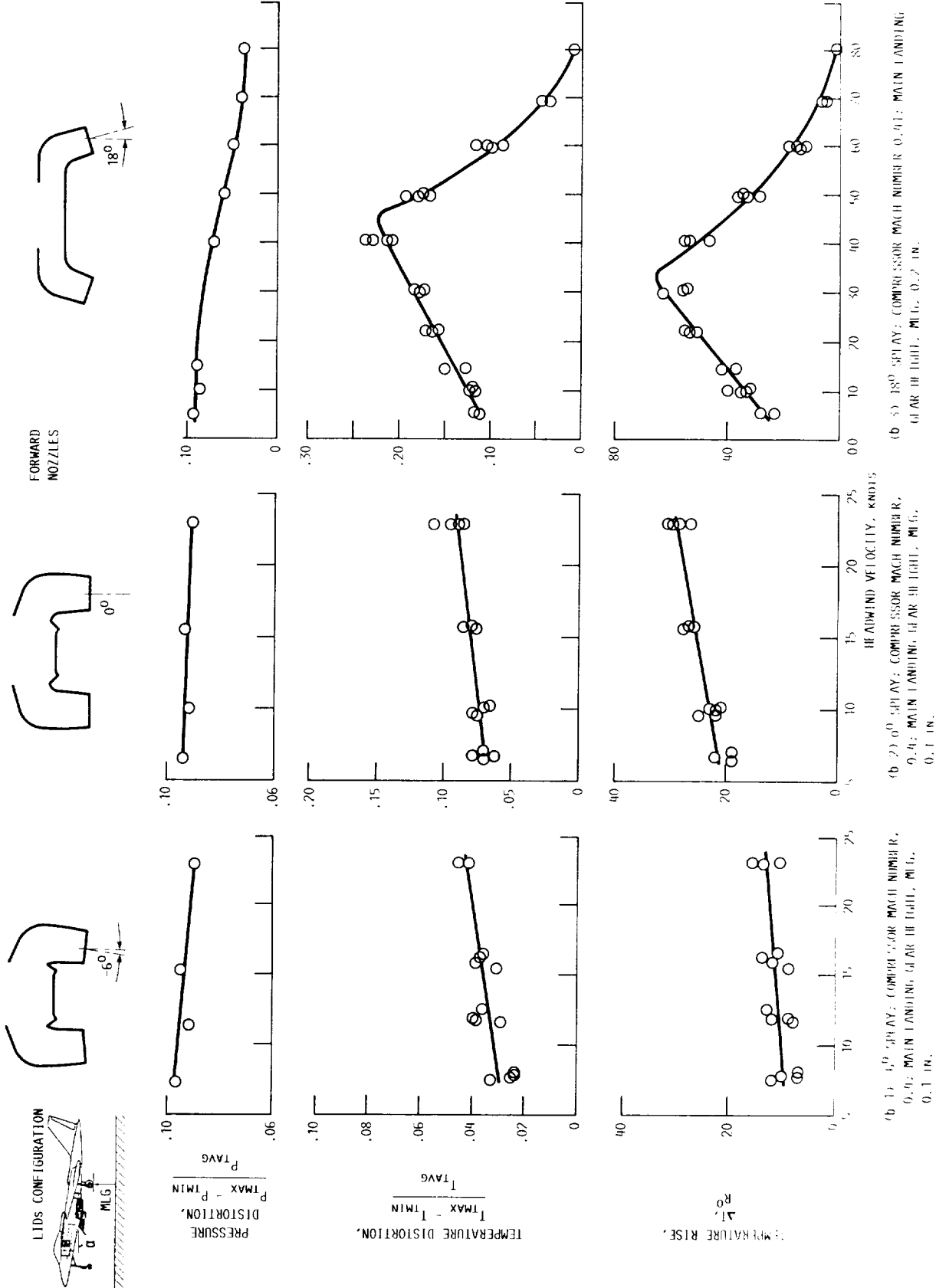
FIGURE 13. - EFFECT OF THE MODEL HEIGHT ABOVE THE GROUND PLANE ON THE COMPRESSOR FACE TEMPERATURE RISE, DESIGN CONDITION. HEADWIND VELOCITY, 10 KNOTS; NOZZLE EXHAUST TEMPERATURE, 960 °R; FORWARD NOZZLE PRESSURE RATIO, 3.02; AFT NOZZLE PRESSURE RATIO, 3.16; COMPRESSOR FACE MACH NUMBER, 0.40; PITCH ANGLE, 6.5°.



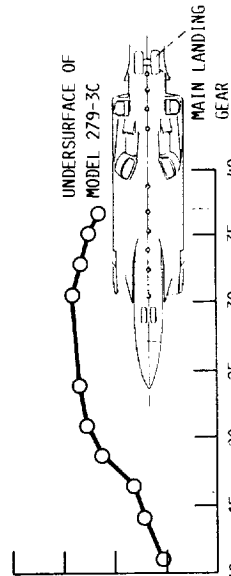
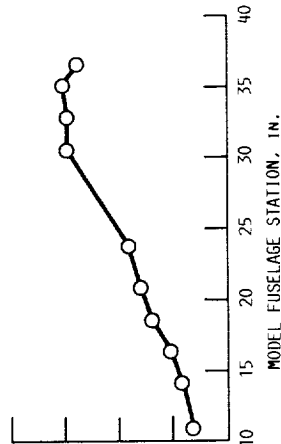
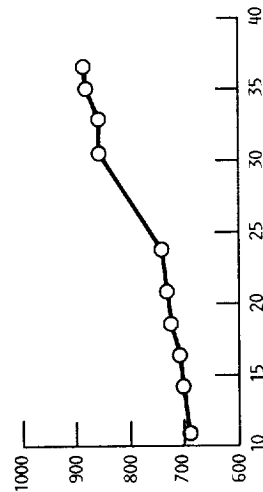
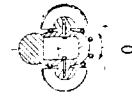
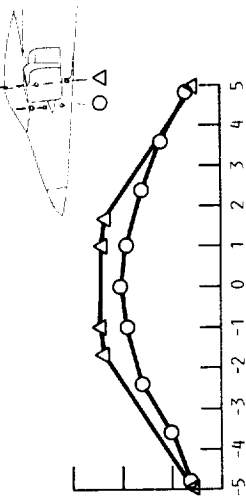
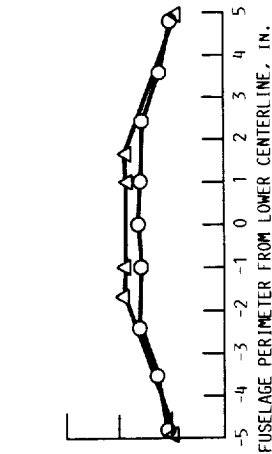
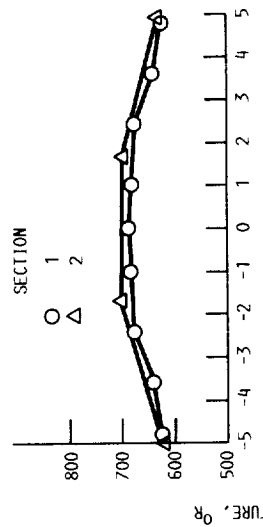
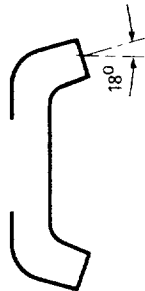
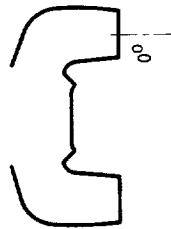
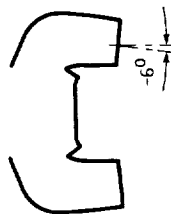
(b) LID's CONFIGURATION.

FIGURE 13. - CONCLUDED.





# FORWARD NOZZLES



(a-1) -6° SPLAY; HEADWIND, 10 KN; COMPRESSOR  
FACE TEMPERATURE RISE, 62 R°; MAIN LANDING  
GEAR HEIGHT, 0.1 IN.

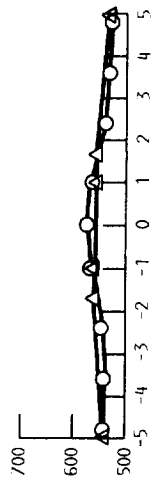
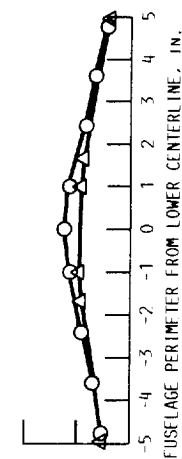
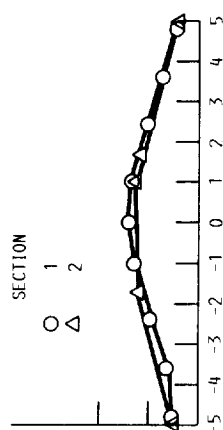
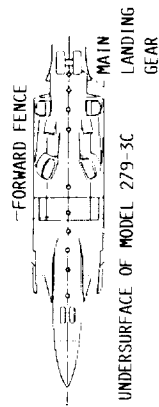
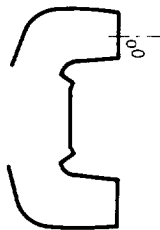
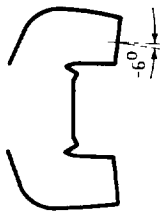
(a-2) 0° SPLAY; HEADWIND, 10 KN; COMPRESSOR  
FACE TEMPERATURE RISE, 82 R°; MAIN LANDING  
GEAR HEIGHT, 0.1 IN.

(a-3) 18° SPLAY; HEADWIND, 10 KN; COMPRESSOR  
FACE TEMPERATURE RISE, 62 R°; MAIN LANDING  
GEAR HEIGHT, 0.1 IN.

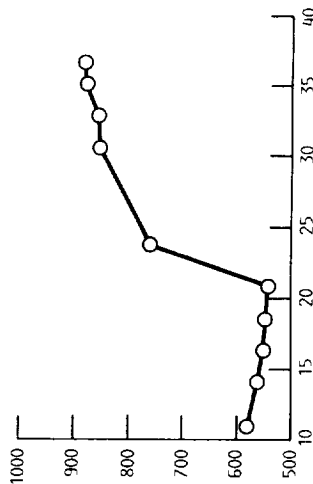
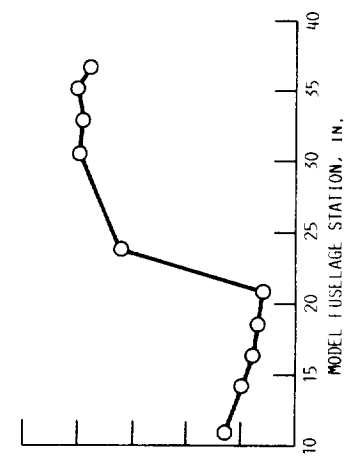
(a) CLEAN CONFIGURATIONS.

FIGURE 15. - EFFECT OF FORWARD NOZZLE SPLAY ANGLE ON THE FUSELAGE TEMPERATURE DISTRIBUTION.

# FORWARD NOZZLES



SURFACE AIR TEMPERATURE, °R



(b-1) -6° SPLAY: HEADWIND, 12 KN; COMPRESSOR FACE TEMPERATURE RISE, 0; MAIN LANDING GEAR HEIGHT, 0.1 IN.

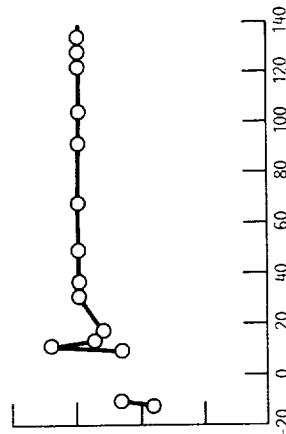
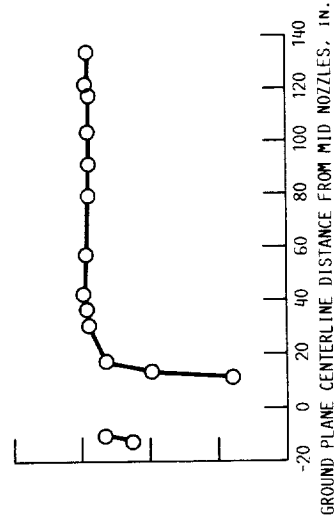
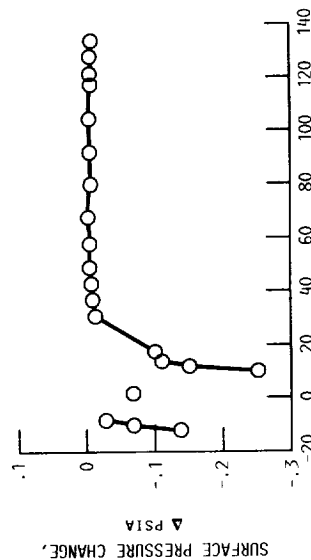
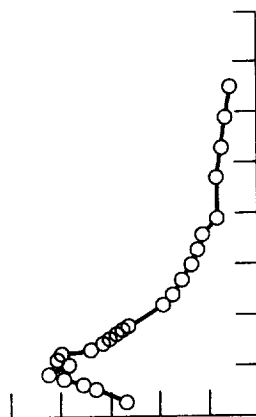
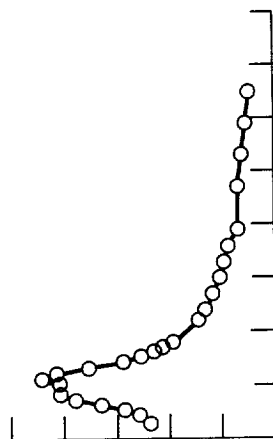
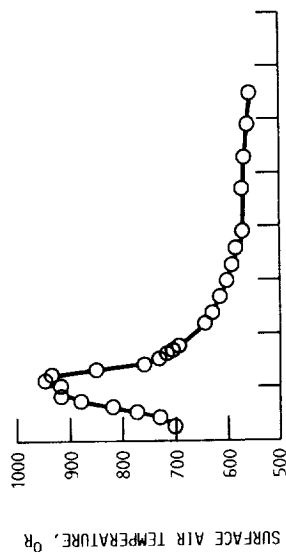
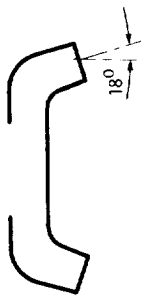
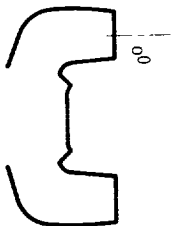
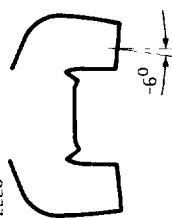
(b-2) 0° SPLAY: HEADWIND, 10 KN; COMPRESSOR FACE TEMPERATURE RISE, 22 R°; MAIN LANDING GEAR HEIGHT, 0.2 IN.

(b-3) 18° SPLAY: HEADWIND, 10 KN; COMPRESSOR FACE TEMPERATURE RISE, 35 R°; MAIN LANDING GEAR HEIGHT, 0.1 IN.

(b) WITH LIDS CONFIGURATIONS.

FIGURE 15. - CONCLUDED.

# FORWARD NOZZLES



(a-1) -6° SPLAY; HEADWIND, 10 KN; COMPRESSOR  
FACE TEMPERATURE RISE, 62 R°; MAIN LANDING  
GEAR HEIGHT, 0.1 IN.

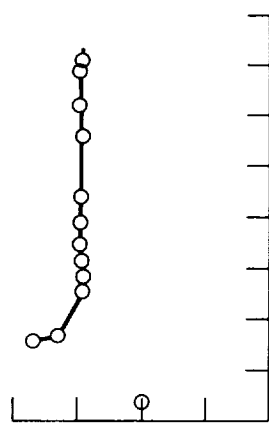
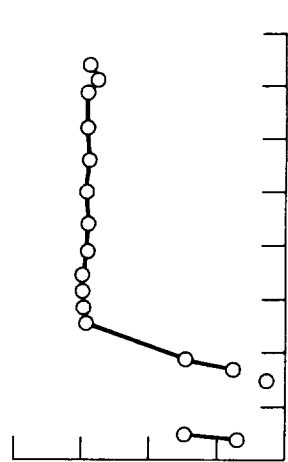
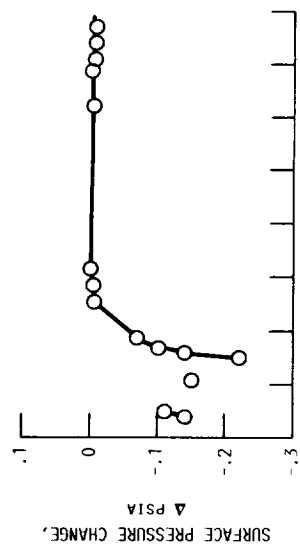
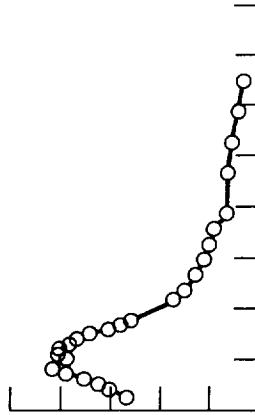
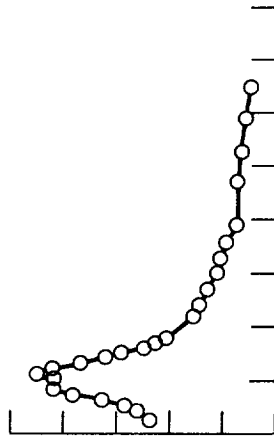
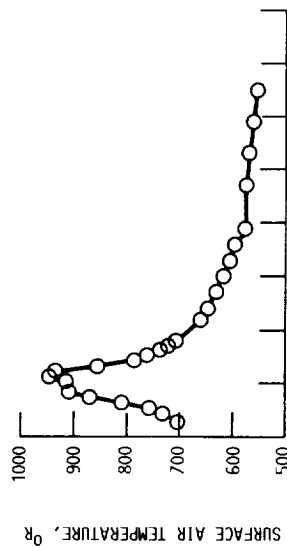
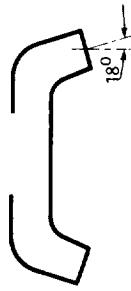
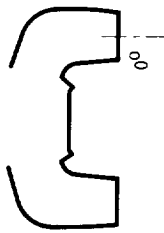
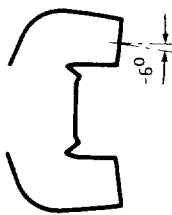
(a-2) 0° SPLAY; HEADWIND, 10 KN; COMPRESSOR  
FACE TEMPERATURE RISE, 82 R°; MAIN LANDING  
GEAR HEIGHT, 0.1 IN.

(a-3) 18° SPLAY; HEADWIND, 10 KN; COMPRESSOR  
FACE TEMPERATURE RISE, 62 R°; MAIN LANDING  
GEAR HEIGHT, 0.2 IN.

(a) CLEAN CONFIGURATION.

FIGURE 16. - GROUND PLANE CENTERLINE TEMPERATURE AND PRESSURE DISTRIBUTIONS AT 10 KNOTS AND DESIGN NOZZLE PRESSURE RATIO.

# FORWARD NOZZLES



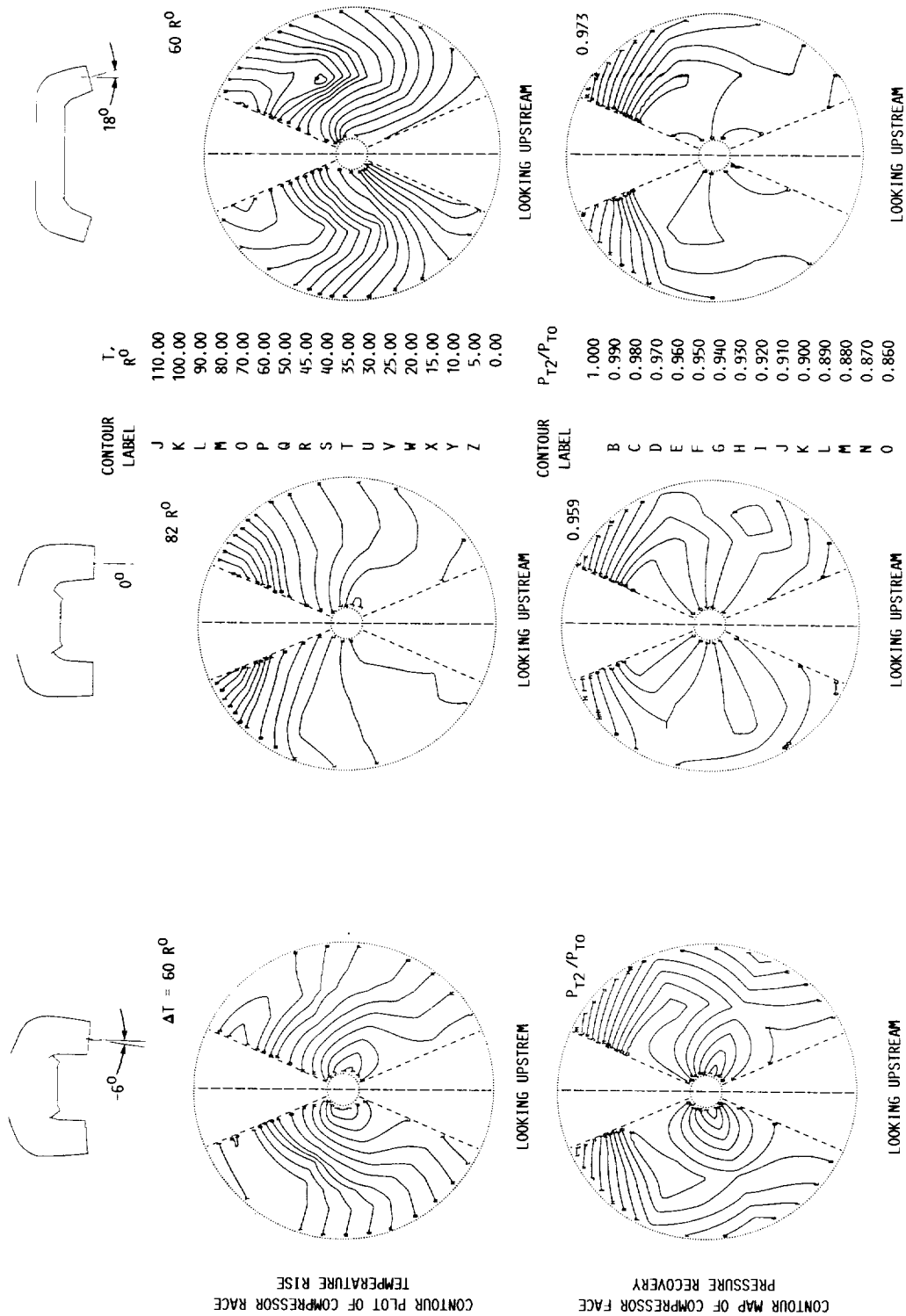
(b-1) -6° SPLAY; HEADWIND, 12 KN; COMPRESSOR  
FACE TEMPERATURE RISE, 0; MAIN LANDING  
GEAR HEIGHT, 0.1 IN.

(b-2) 0° SPLAY; HEADWIND, 10 KN; COMPRESSOR  
FACE TEMPERATURE RISE, 22 R°; MAIN LANDING  
GEAR HEIGHT, 0.1 IN.

(b-3) 18° SPLAY; HEADWIND, 10 KN; COMPRESSOR  
FACE TEMPERATURE RISE, 35 R°; MAIN LANDING  
GEAR HEIGHT, 0.2 IN.

(b) WITH LIDS CONFIGURATIONS.

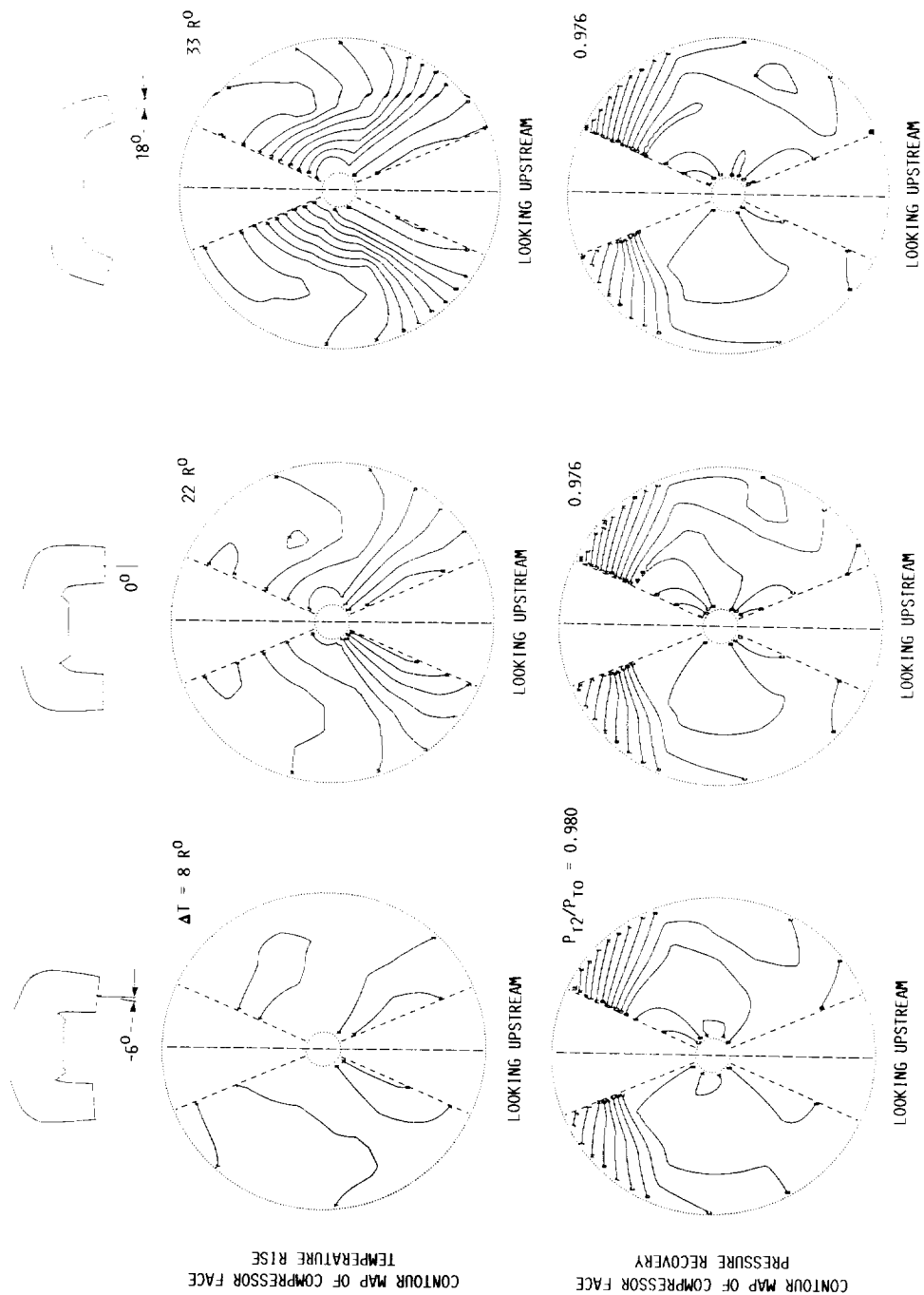
FIGURE 16. - CONCLUDED.



(a) CLEAN CONFIGURATIONS.

FIGURE 17. - EFFECT OF FORWARD NOZZLE SPRAY ANGLE ON THE COMPRESSOR FACE TEMPERATURE RISE AND PRESSURE RECOVERY.





(b) WITH LIDS CONFIGURATIONS.  
FIGURE 17. - CONCLUDED.



National Aeronautics and  
Space Administration

## Report Documentation Page

1. Report No. NASA TM-102358 AIAA-89-2910		2. Government Accession No.		3. Recipient's Catalog No.	
4. Title and Subtitle Engine Inlet Distortion in a 9.2 Percent Scale Vectored Thrust STOVL Model in Ground Effect				5. Report Date	
				6. Performing Organization Code	
7. Author(s) Albert L. Johns, George Neiner, J.D. Flood, K.C. Amuedo, and T.W. Strock				8. Performing Organization Report No. E-5072	
				10. Work Unit No. 505-62-71	
9. Performing Organization Name and Address National Aeronautics and Space Administration Lewis Research Center Cleveland, Ohio 44135-3191				11. Contract or Grant No.	
				13. Type of Report and Period Covered Technical Memorandum	
12. Sponsoring Agency Name and Address National Aeronautics and Space Administration Washington, D.C. 20546-0001				14. Sponsoring Agency Code	
15. Supplementary Notes Prepared for the 25th Joint Propulsion Conference cosponsored by the AIAA, ASME, SAE, and ASEE, Monterey, California, July 10-12, 1989. Albert L. Johns and George Neiner, NASA Lewis Research Center; J.D. Flood, K.C. Amuedo, and T.W. Strock, McDonnell Aircraft Company, McDonnell Douglas Corporation, St. Louis, Missouri.					
16. Abstract Advanced Short Takeoff/Vertical Landing (STOVL) aircraft which can operate from remote locations, damaged runways, and small air capable ships are being pursued for deployment around the turn of the century. To achieve this goal, NASA Lewis Research Center, McDonnell Douglas Aircraft, and DARPA defined a cooperative program for testing in the NASA Lewis 9- by 15-Foot Low Speed Wind Tunnel (LSWT) to establish a database for hot gas ingestion, one of the technologies critical to STOVL. This paper will present results showing the engine inlet distortions (both temperature and pressure) in a 9.2% scale Vectored Thrust STOVL model in ground effects. Results are shown for the forward nozzle splay angles of 0°, -6°, and 18°. The model support system had 4 degrees of freedom, heated high pressure air for nozzle flow, and a suction system exhaust for inlet flow. The headwind (freestream) velocity was varied from 8 to 23 kn.					
17. Key Words (Suggested by Author(s)) STOVL; Hot gas ingestion; Temperature distortion; Pressure distortion; Wind tunnel testing				18. Distribution Statement Unclassified - Unlimited Subject Category 02	
19. Security Classif. (of this report) Unclassified		20. Security Classif. (of this page) Unclassified		21. No of pages 24	
				22. Price* A03	